*Asian Journal of Physical and Chemical Sciences*

*3(2): 1-12, 2017; Article no.AJOPACS.36403*
*ISSN: 2456-7779*

# Synthesis, Characterization and Thermoluminescence Properties of Rare Earth Ions Doped Silica Glass Prepared by Sol-Gel Technique

**Fawzeia Khamis[1*] and Dia-Eddian Arafah[2,3]**

*[1]University of Tripoli, Department of Physics, Tripoli 13220, Libya.*
*[2]Al al-Bayt University, P.O.Box 130040, Mafraq 25113, Jordan.*
*[3]Department of Physics, The University of Jordan, Amman 11942, Jordan.*

***Authors' contributions***

*This work was carried out in collaboration between both authors. Both authors designed the study. Author FK preformed the statistical analysis, wrote the protocol and wrote the first draft of the manuscript. Both authors managed analysis of study and managed the literature searches. Both authors read and approved the final manuscript.*

***Article Information***

DOI: 10.9734/AJOPACS/2017/36403
Editor(s):
(1) Kuldeep Kholiya, Department of Applied Science, B. T. Kumaon Institute of Technology, Dwarahat, India.
Reviewers:
(1) Omojola Akintayo Daniel, Federal Medical Centre Asaba, Nigeria.
(2) Yong Gan, California State Polytechnic University, USA.
(3) Netra Pal Singh, Meerut College, India.
Complete Peer review History: http://www.sciencedomain.org/review-history/21153

***Original Research Article***

***Received 27th August 2017***
***Accepted 15th September 2017***
***Published 26th September 2017***

## ABSTRACT

**Aims:** The main aim of this work is to synthesize the silica glass ($SiO_2$-glass) samples doped with different rare earths (RE) and then to study the thermoluminescence (TL) glow curve of these samples.
**Study Design:** Rare earth doped samples namely silica glass ($SiO_2$-glass) are synthesized by the sol-gel technique.
**Place and Duration of Study:** Department of Physics (Atomic Physics Lab's, The University of Jordan), between May 2012 to May 2014.
**Methodology:** This work presents a study of the role of an external impurities, namely dysprosium (Dy) and europium (Eu) with different concentrations on the mechanism of TL in $SiO_2$-glasses.
**Results:** The study of the best concentration for each doped silica, the basic TL feature main glow peaks occur in 156-320°C for $Eu^{3+}$(0.2 mol%) and 159-300°C for $Dy^{3+}$(0.002 mol%) with heating

**Corresponding author: E-mail: fawzeiak@yahoo.com, khamesf@gmail.com;*

rate 2°C/s . At all β-dose levels, the intensities of the peaks are nearly linear in the dose range of o.5-2Gy. The fading rate of the $SiO_2$: Dy(0.002 mol%) response at room temperature is small. Variations of the normalized TL intensity as function of heating rate indicated reduction of TL-response accompanied by shift of TL-peaks towards higher temperatures. The kinetic parameters (activation energy E, frequency factors s) of all phosphors are determined and compared using two methods, with correlation of the trapping states to structure and comparison with values available from the literature.

**Conclusion:** Rare earth doped $SiO_2$-glass phosphors were successfully synthesized by sol-gel technique. Among all the dopants Dy(0.002 mol%) doped $SiO_2$-glass phosphor showed the high intense and high temperature glow peaks (156°C up to 315°C) with good glow curve shape. In the case of $SiO_2$-glass,Eu doped phosphor has given the good glow curve shape with glow curve structure. The glow peak of $SiO_2$: $Eu^{3+}$ is situated at 152°C.

*Keywords: Thermoluminescence; silica glass; sol-gel; $E'$-centers; trapping parameters.*

## 1. INTRODUCTION

Rare earth (RE) ions doped silica glass prepared by sol-gel technique are of interest for various applications including solid sate lasers, optical waveguides and fiber amplifiers [1,2]. This is due to their excellent transparency over a wide spectral region, good chemical and mechanical properties, and high radiation hardness. Presently, most of RE-doped silica glasses for optical applications are prepared by sol-gel method. A high doping level of RE ions in silica glass with minimal formation of clusters of RE ions can be achieved by sol-gel processes [3]. With a high doping concentration, RE and other metal ions have a strong tendency to form clusters in sol gel silica as well [3-7]. At low concentration levels, the RE ions can be distributed homogeneously in a tetrahedral network with the formation of Si-O-RE structure. However, with an increasing concentration and due to strong interaction between the RE ions and oxygen ions, RE-O-RE clusters may form, and eventually lead to phase separation [3,8]. Among the several techniques used to examine the defect behaviors is the well known technique known as thermoluminescence (TL), through which a good deal of information can be obtained from analysis of the glow curves. Several papers have been published on the TL of pure and doped silica glass with specific reference to TL dating [9-11]. Nevertheless, some common features are found in most of the glow curves of quartz, silica and $SiO_2$ films [12-13], and analogues similarities have been observed in the emission bands in the TL of these materials [14]. Among the common features of the TL of ordered crystalline and amorphous silica glass is a peak at about 100-150°C [9-11]. The sol-gel technique that is used to synthesis highly homogeneous glass at comparatively low temperatures (900-1100°C) is attracting much attention as a synthesizing technique for optical fiber pre-forms [15-18]. In this paper we describe the synthesis of a rare earth doped silica glass using sol-gel technique, and present preliminarily results of a beta radiation detection using the thermoluminescence enhancement of the RE excited states.

## 2. EXPERIMENTAL

Samples were prepared using the sol-gel method as described elsewhere [11,19]. Samples were synthesized from the starting solution, tetraethyloxysilane (TEOS), with molar ratio: (TEOS:$C_2H_5OH$:$H_2O$:HF) equals to: (1:4:4:0.05). The solution was mixed and stirred well for about 1 hour at ambient temperature, using a magnetic stirrer, until it became transparent. For preparing the REs doped silica, (among, RE ions, europium chloride and dysprosium oxide with different concentrations), molar ratios were also added to the starting solution and then stirred until the solution became transparent, after about 1hour. the solution, which was placed into a cylindrical container and covered with an aluminum foil, was held at 60°C for about 24h. The container was dipped into a water bath that was held at 60°C for 24h to favor the polymeric route over the colloidal one, and induces hydrolysis and condensation, the period at which the volume becomes about one third of its original volume. The dry gel obtained was then sintered in an electric oven at 200°C/2h and was then slowly cooled down and brought to room temperature (RT).

The resulting homogeneous mix prepared from sol-gel technique was in the form of coarse grained particles. The powder was grinded using a mortar and sieved using a mesh of particle size less than ≤ 75 μm. Samples used in the

measurements were shaped out in the form of circular discs, each of mass 15 mg, and pressed under a 1.0 ton pressure with dimensions: 4.5mm diameter and thickness about 1 mm. All samples were then annealed at different temperatures up to 1100°C in a platinum (Pt) crucible for 2 h using a microprocessor controlled furnace and then cooled slowly to RT prior to irradiation.

Irradiations were carried out at RT with a calibrated $^{90}$Sr-$^{90}$Y-source by β-particles using VINTEN Model 623 automatic dosimeter irradiator of nominal activity 1 mCi which, delivers to the samples dose at a rate of 2.87μGy $s^{-1}$. The temperature variation in the range from ambient to 673 K was 2 K. This test dose was found suitable for stability conditions and repeated measurements indicate that the annealing temperature results in the detected GL-peaks. The delivered test dose to the samples was varied up to 2Gy, in steps of 0.5Gy. This test dose was, however, found to reveal all GL-peaks in the GL-curve of sample type prepared by sol-gel technique. The read out stage was made using Harshaw Model 3500 TLD reader, with planchet heating system controlled by Windows®–based Radiation Evaluation and Management System (Win-REMS), a proprietary of Thermo Electron Corporation RM&P's, operating on a personal computer and connected to the Reader via a serial port [20]. The TL-signal representing the Glow (GL-) curves were recorded using suitable software, Win-REMS, interfaced to a personal computer (PC), for further analysis. All GL-curves were read using a linear heating rate of 2°$Cs^{-1}$, from room temperature up to 380°C with preheat temperature set at 80°C, to eliminate the more rapidly fading low temperature peaks in the GL-curves and to see end of signal (spectrum). This, however, ensures consistency within our measurements, except for those varying heating rate experiments where, constant but varied heating rates between 2 and 10°$Cs^{-1}$ were used. More details about the preparation procedure and conditions of the sol-gel method and the measurement system are found elsewhere [19,21].

## 3. RESULTS AND DISCUSSION

### 3.1 Effect of Concentrations of Each Doped $RE^{3+}$ on Glow Curve

The starting concentration for the doping process was 0.1mol%, according to Pandy et al. 2004 method, for the $Eu^{3+}$ samples. Other concentrations, namely (0.2) and (0.3) mol% were used; while (0.0002, 0.0003, 0.001, 0.002, 0.01, 0.03 and 0.05 mol%) of $Dy^{3+}$ions; with all samples were annealed at $1100^{o}C/2h$. Figs. 1-2 show the glow curves (GL-curves) of samples of doped with $Eu^{3+}$ and $Dy^{3+}$, respectively at different concentrations were recorded using a linear heating rate of 2$Ks^{-1}$, also readout after irradiation of 2Gy. The resulting GL-curve was found to exhibit the highest intensity for TL-peaks. It is interesting to note that the dopant not only resulted in the detection of the new and high temperature TL-peaks, but also enhancement on the TL-response of the main dosimetric peak was noted. The shape of glow curve is different with doped-$SiO_2$, becomes same of the best concentrations for each Eu(0.2 mol%) and Dy(0.002 mol%), but results in a lower TL-response and forms a sharp peak around 430K and the highest intensity for TL-peaks, whereas the intensity is about 5-times in comparison with doped Eu(0.2 mol%) samples. They are emphasized that each of these doped samples were de-convoluted to the same number of peaks, in addition to a background signal. Such quantitative measures make the novel doped material excellent candidate to be used in dosimetry that requires high temperatures working environments. In any case, the kinetic parameters for each GL-curve are listed in Table 1 for comparison and completeness.

### 3.2 Effect of $RE^{3+}$ Doping on the Glow Peak Positions

Fig. 3 shows the effect of the best doped rare earth on the glow curve peak of $SiO_2$: Eu(0. 2 mol%) and Dy(0.002 mol%) comparison with the glow curve of $SiO_2$ only. And Table 2 illustrates the effect of rare earth size on the glow curve peak position of $SiO_2$: Eu(0.2 mol%) and Dy(0.002 mol%). The amount of lattice distortion increases with increasing the size difference between the RE ion and the substituted ion and with additionally the need fulfill for charge compensation. The strategy taken by the lattice to minimize the strain is that the RE ions associate in pairs or larger clusters with lattice defects and structural distortions into relatively large defect complexes. A TL model [23] that links the RE ions sizes will strongly influence the trap stability resulting in TL peaks which differ in temperature in a systematic way depending on the ionic size of the RE dopants. For $SiO_2$: RE, both glow peaks movement in the same way with ionic radius with sift up to 50K for peaks at high temperature and to 63K for low temperature were

observed, as [24]. Conversely, the low temperature data from alkaline earth fluorides [25] indicate that the peak positions are insensitive to the RE ion and no general trend emerges for high temperature data.

### 3.3 Structural Analysis of The Best Concentration of Each Doped Eu(0.2mol%) and Dy(0.002mol%)

Fig. 4 shows XRD patterns of 0.2mol% $EuCl_3$ in (a) and 0.002mol% $Dy_2O_3$ in (b) doped silica gel at RT and annealed at and $1100^oC/2h$. The two figures illustrate the effect of the annealing temperature ($T_a$) on the structure. The peaks exhibit a shift to lower angles with increase of the annealing temperature. In both the cases, only broad diffraction peaks were observed. The broadness of these peaks indicates the amorphous nature of the glassy phase. The beta rays irradiation caused partial transformation from amorphous to crystalline. The $Eu^{3+}$and $Dy^{3+}$ activators ions did not contribute to any diffraction peaks suggesting that the ions are well dispersed in the silica matrix because of their relatively low concentration. The crystallites size are noticed to change with the $T_a$; as the $T_a$ increased, the particle size tended to increase too, as shown in Table 3. This is also, consistent with the fact that larger size particles result in a better efficiency; and when compared to collecting light in, e.g. solar cells. Fig. 5 shows the SEM monograph and EDS spectrum of 0.2mol% $EuCl_3$ doped $SiO_2$ powders and annealed at $1100^oC/2h$. The analyses of EDS spectra reveals the following ratios: 48.27wt%, 43.39wt% and 8.34wt% for Si, O and $Eu^{3+}$, respectively.

**Table 1. Trapping parameters of $SiO_2$: $Eu^{3+}$ (0.2 mol%) as obtained from numerical fitting technique at a heating rate 2Ks$^{-1}$**

| Con. (mol%) | Ps | E(eV) | $T_m$(K) | b | s(s$^{-1}$) | *τ |
|---|---|---|---|---|---|---|
| Eu (0.2) | $P_1$ | 0.90 | 398 | 1.00 | $3.29\times10^{10}$ | 1.36d |
| | $P_2$ | 1.07 | 425 | 1.23 | $6.61\times10^{11}$ | 2.00m |
| | $P_3$ | 1.23 | 447 | 1.30 | $1.04\times10^{13}$ | 6.15y |
| | $P_4$ | 1.44 | 478 | 1.25 | $2.20\times10^{14}$ | $1.26\times10^{3}$y |
| | $P_5$ | 1.75 | 504 | 1.63 | $4.9\times10^{16}$ | $13.19\times10^{5}$y |
| | $P_6$ | 1.78 | 548 | 1.42 | $3.16\times10^{15}$ | $67.67\times10^{6}$y |
| | $P_7$ | 1.98 | 593 | 2.5 | $8.17\times10^{15}$ | $7.62\times10^{10}$y |
| Dy (0.002) | $P_1$ | 0.93 | 430 | 1.10 | $9.28\times10^{9}$ | 15.96d |
| | $P_2$ | 1.09 | 456 | 1.28 | $1.33\times10^{11}$ | 21.93m |
| | $P_3$ | 1.33 | 487 | 1.44 | $7.36\times10^{12}$ | 467.29y |
| | $P_4$ | 1.40 | 522 | 1.55 | $3.79\times10^{12}$ | $14.8\times10^{4}$y |
| | $P_5$ | 1.68 | 570 | 2.5 | $7.9\times10^{13}$ | $5.02\times10^{7}$y |

*with, Std-Error of: E= ±0.06%, $T_m$= ±5%, b= ±0.03% lifetime measurements are determined at ambient temperature ($18^oC$), and scale is in years unless specified otherwise, with (d=days and m=months).*

**Table 2. The ionic radius of the RE ions with the peak maxima of the low and high- temperature peaks**

| Undoped RE- ion | Ionic radius ($A^o$) | $T_m$(K) of the low-temp. peaks | $T_m$(K) of the high-temp. peaks |
|---|---|---|---|
| | -- | 423 | 580 [22] |
| Dy | 0.912 | 430-493 | 530-573 |
| Eu | 0.947 | 423-486 | 543-591 |

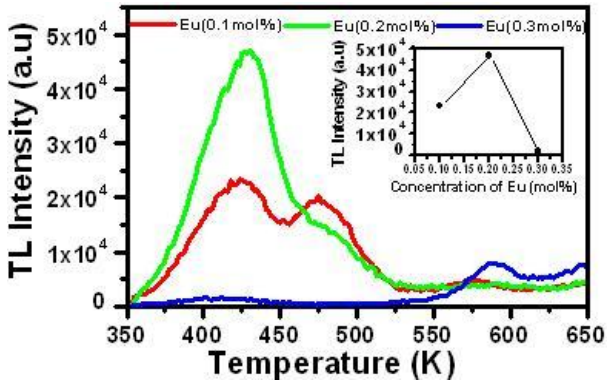


**Fig. 1. TL glow curves of $SiO_2$: $Eu^{3+}$ with different concentrations irradiated with 2Gy after annealing at $1100^oC/2h$ at a heating rate of $2Ks^{-1}$**

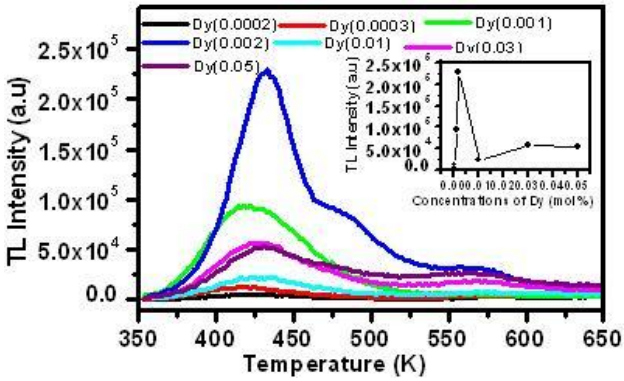


**Fig. 2. TL glow curves of $SiO_2$: $Dy^{3+}$ with different concentrations irradiated with 2Gy after annealing at $1100^oC/2h$ at a heating rate of $2Ks^{-1}$**

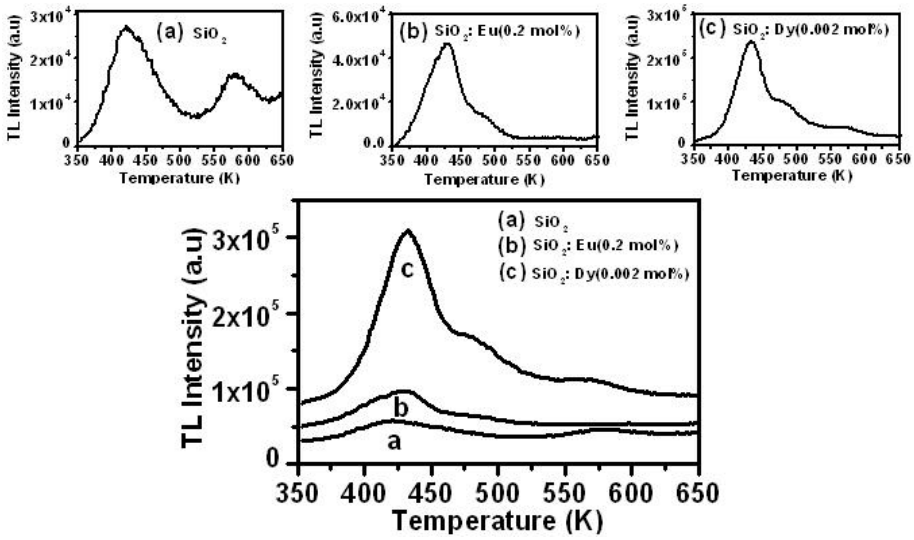


**Fig. 3. Beta irradiated TL glow curves of undoped $SiO_2$ and doped with different rare earths annealing at $1100^oC/2h$ at a heating rate of $2Ks^{-1}$**

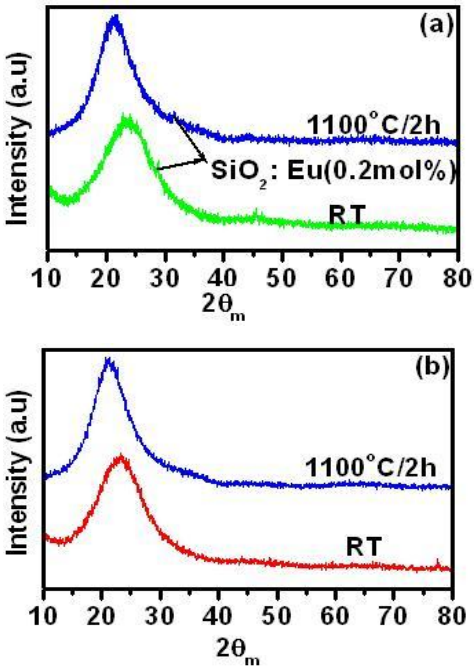


**Fig. 4. XRD pattern of $SiO_2$ doped with: (a) 0.2 mol% $EuCl_3$ and (b) 0.002 mol% of $Dy_2O_3$ after annealing at $1100^oC/2h$**

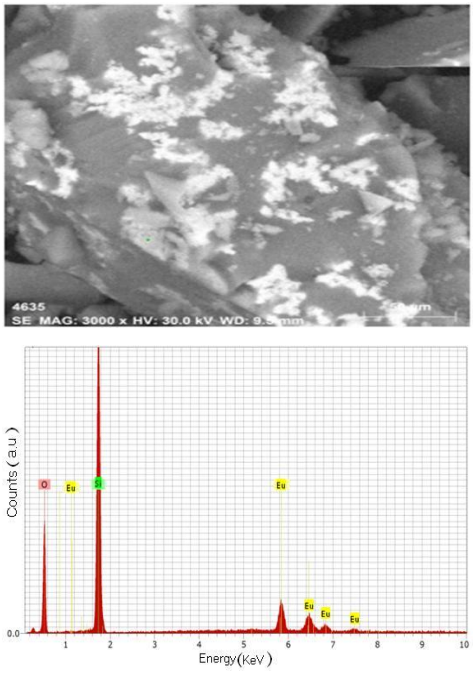


**Fig. 5. SEM image (upper) and EDS spectrum (lower) of amorphous $SiO_2$: $Eu^{3+}$ (0.2 mol%) annealed at $1100^oC/2h$, obtained with magnification, 1600. Peaks are labeled in accordance with the main elements present in the sample**

### 3.4 Effect of Irradiation Dose of $SiO_2$: $RE^{3+}$ Ions for The Best Concentrations of Each $Eu^{3+}$ and $Dy^{3+}$

Figs. 6(a, b) show the dose response of TL intensity of $SiO_2$: $Eu^{3+}$ (0.2 mol%), $Dy^{3+}$ (0.002 mol%) samples. The TL intensity increases with the β-irradiation dose exposure up to 2Gy and becomes saturated after 2Gy β-irradiation in both the materials. A close look at Figs. 7(a,b), indicate the tendency of doped $SiO_2$ to show a linear behavior with the irradiation dose. This important result emphasizes that the material after doping could be used to detect radiation. It is worth mentioning that such a linear behavior can also be generalized to the main dosimetric peaks: $P_1$, $P_2$ and $P_3$ extracted from the GL-curves. Considering the main TL-peak, namely $P_1$, it was also observed that the sensitivity of doped Dy samples is about five times higher than that found by doped Eu of main peak $P_1$. The region between 475 and 600K is, however, complex and contains satellite broad peaks that need further investigations.

### 3.5 Effect of Heating Rate on Glow Curve of $SiO_2$: $RE^{3+}$ Ions for The Best Concentrations of Each $Eu^{3+}$ and $Dy^{3+}$

Fig. 8 shows TL glow curves of silica glass samples doped with $Eu^{3+}$ (0.2mol %) in (a), and $Dy^{3+}$ (0.002mol %) in (b), irradiated to a dose of 2Gy and readout at different heating rates from 2 up to $10Ks^{-1}$. Based on Fig. 8, it is clear that the temperature $T_m$ corresponding to the maximum intensity of the main glow peak exhibits a tendency to shift to higher of temperatures with the increase of the heating rate, β. The TL intensity must therefore be normalized to the heating rate used ($TL/\beta$). If this normalization is done, the correct representation is obtained which indicates a decreasing behavior of the silica glass doped $Eu^{3+}$ and $Dy^{3+}$ as a function of increasing the heating rate; a phenomenon that is frequently observed in practice when dealing with TL. It has been explained through a thermal quenching effect [26]. Figs. (9,10) display the de-convoluted emission peaks of $SiO_2$: $Eu^{3+}$ and $Dy^{3+}$. The emission peaks of each sample and the change in peak positions with heating rate

are shown in Fig. 11. The kinetics effects on the parameters values at 2 heating rate as example are listed in Table 1.

From Table 1 one notices variations on the parameters as a result of different a heating rates. For all peaks, an increase in the activation energy values, which indicates that the defects in the sample become deeper with a probability of increasing the efficiency of trapping more electrons, is noticed. One also notices that activation in terms of the b values where for $P_1$ it exhibits direct recombination for the electrons (b $\approx$ 1) while for the other peaks, at different heating rates, a general order kinetic equation is obtained. The initial charge concentration of filled traps ($n_0$) appear to decrease with, increasing the heating rate, while the glow peaks intensity at maximum shows a decrease in intensity as the heating rate is increased with the peak temperature at maximum moving towards higher temperature values; but not in peak1 which shows a small increase followed by a decrease and increases again as the heating rate is increased. This behavior is difficult to explain because of the complex TL mechanism of recombination defects [27]. One may possibly think in terms of the heating rate occurring during the time of reaction is slightly less at low than at high heating rates, and then the peak integral area of an entire glow curve increases with heating rate [28]. The glow curves analyzed by variable heating rate method (VHR) method for the main peaks of $SiO_2$: Eu(0.2 mol%), Dy(0.002 mol%) are shown in Fig. 12 and Table 4 shows E , s and τ values as determined by the VHR, also confirm our findings.

### 3.6 TL Fading of Silica Glass Doped RE

It may appear desirable that the fading patterns of other RE-doped $SiO_2$ in comparison with SiO2: Dy need to be discussed. However, since both of the best concentration of each Eu and Dy dopants produce the same general shape of glow curves with minor differences in the position

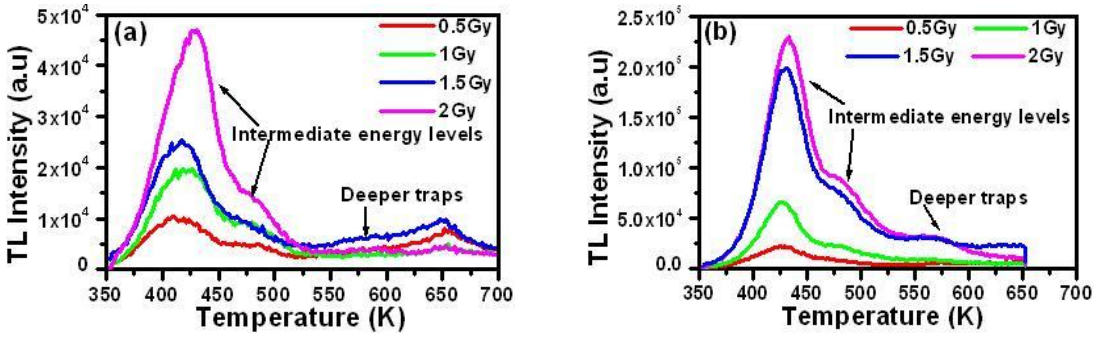


**Fig. 6. GL-curves of SiO2: $RE^{3+}$ are measured at a constant heating rate $2Ks^{-1}$ after irradiation up to 2 Gy. (a) $Eu^{3+}$ (0.02 mol%) and (b) $Dy^{3+}$ (0.002 mol%)**

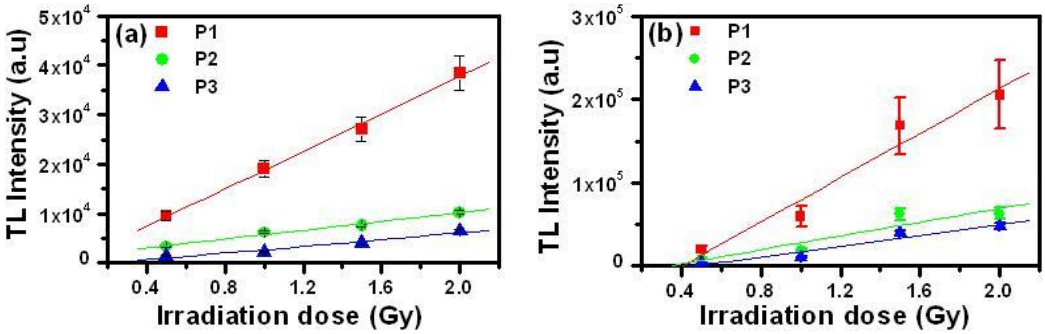


**Fig. 7. TL response of different extracted peaks plotted against irradiation dose for $SiO_2$ doped with: (a) $Eu^{3+}$(0.2 mol%) and (b) $Dy^{3+}$(0.002 mol%)**

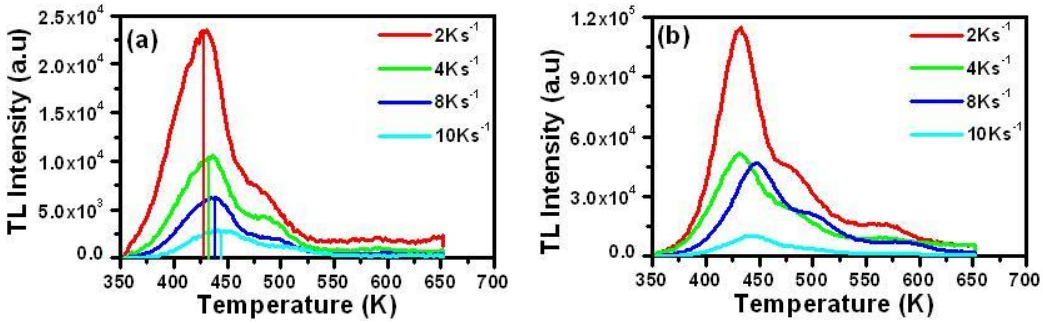


**Fig. 8. Normalized TL intensity of GL-curves of $SiO_2$ doped with: (a) $Eu^{3+}$ (0.2 mol%) and (b) $SiO_2$: $Dy^{3+}$ (0.002 mol%), obtained at different heating rates**

of the dosimetric peak, there is no reason to suspect that different RE ions will produce different fading patterns. Fading mainly depends on the host material and preparation method [29]. In addition, from the viewpoint of the energy transfer model, the RE ion is completely separated from the trapping sites. The RE receives the recombination energy resonantly and re-emits it as a TL. Therefore, carrying out fading measurements on other Eu ion will not produce fading patterns appreciably different that obtained for Dy as a representative ion for the Eu.

Since it may take some time after a radiation accident has occurred before an access to the glass is possible, a desirable and crucial property of the glass that must be studied is, fading. This is the property that tells for how long a material can hold any signal stored in it. Fading of $SiO_2$: Dy(0.002 mol%) samples was studied after imparting a test dose of 2Gy after annealed at $1100^{o}C/2h$ at storage temperature of $18^{o}C$ . Some samples of these were readout immediately. Others were kept at room temperature for a later time. Some of these were read at the response against delay time is shown

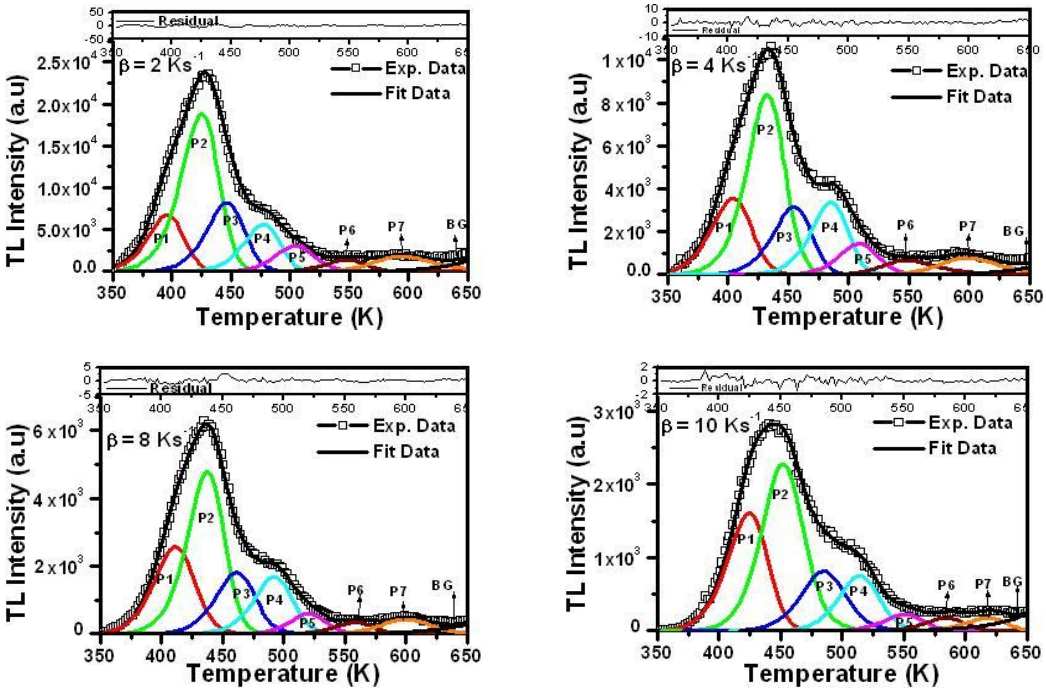


**Fig. 9. De-convolution of normalized GL-curves of $SiO_2$ doped with $Eu^{3+}$(0.2 mol%) and obtained at different heating rates**

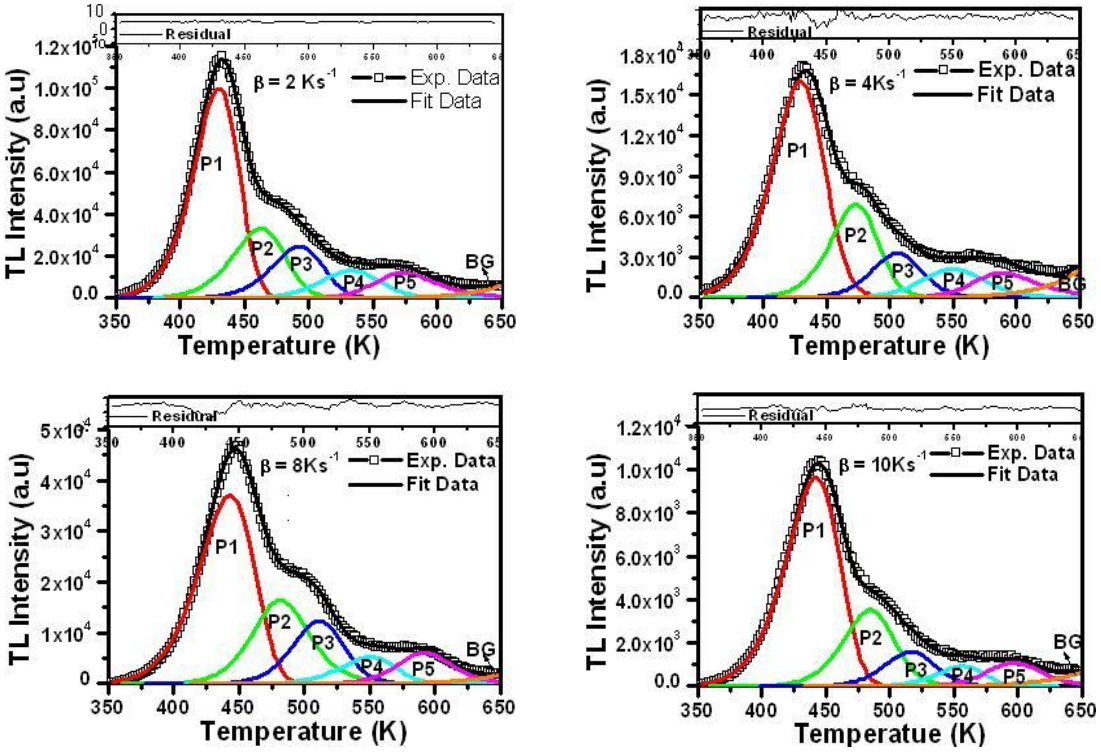


**Fig. 10. De-convolution of normalized GL-curves of $SiO_2$ doped with $Dy^{3+}$(0.002 mol%) and obtained at different heating rates**

Fig. 13. The figure shows an initial high fading rate followed by a slower rate at longer times, which is a characteristic of anomalous fading in contrast to thermal and optical fading. Anomalous fading, however, is believed to arise from quantum tunneling of the trapped charge to recombination center or to arise from localized transitions within the defects complex. No changes in the GL-curve shape with storage time are observed up to 100 days.

**Table 3. The crystallite size of $SiO_2$: $Eu^{3+}$ and $Dy^{3+}$ prepared by sol-gel at RT and annealed at $1100^oC/2h$**

| XRD-Analysis of | Position of angle ($2\theta_m$) | | FWHM-β(radians) | | Crystallite Size [$D=0.9\times\lambda/\beta\times\cos(\theta_m)$]($A^o$) | |
|---|---|---|---|---|---|---|
| | RT | 1100°C/2h | RT | 1100°C/2 h | RT | 1100°C/2h |
| Eu(0.2)mol% | 23.58 | 21.31 | 12.37° (=0.22) | 8.46° (=0.15) | 6.45 | 9.41 |
| Dy(0.002)mol% | 23.79 | 21.29 | 11.08° (=0.19) | 8.86° (=0.15) | 7.46 | 9.41 |

**Table 4. Values of the activation energy E (eV), frequency factor s ($s^{-1}$) and lifetime τ of main dosimetric peaks of both silica glasses determined by the VHR**

| Main Peak | $SiO_2$: Eu(0.2 mol%) | | | $SiO_2$: Dy(0.002 mol%) | | |
|---|---|---|---|---|---|---|
| | E (eV) | s ($s^{-1}$) | *τ | E (eV) | s ($s^{-1}$) | *τ |
| $P_1$ | 2.11 | $1.26\times 10^{20}$ | $8.82\times 10^{8}$y | 1.65 | $2.65\times 10^{14}$ | $4\times 10^{6}$y |

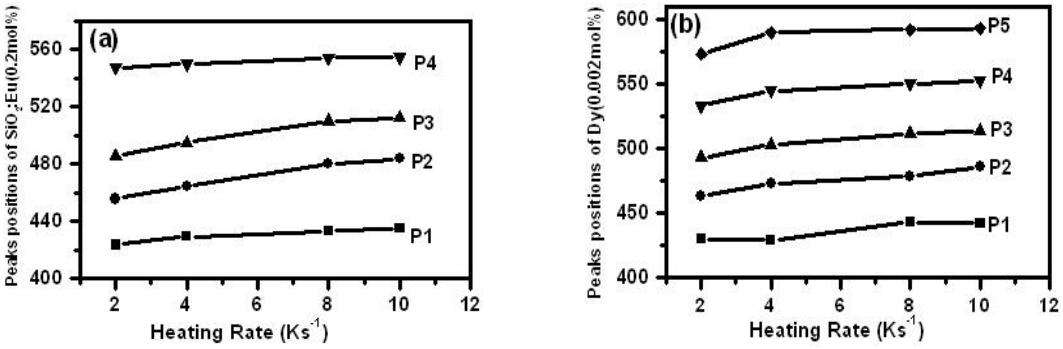


**Fig. 11. Peak maximum temperature of glow peaks as a function of the heating rate. (a) $SiO_2$: $Eu^{3+}$ (0.2 mol%), (b) $SiO_2$: $Dy^{3+}$ (0.002 mol%).**

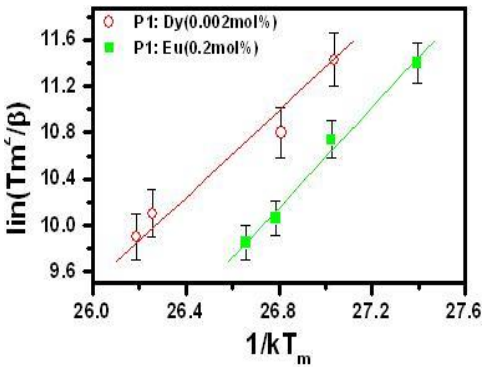


**Fig. 12. Plots of $\ln(T_m^2/\beta)$ against $1/kT_m$ of $SiO_2$ samples using VHR with, (0.2 mol%) $Eu^{3+}$ (solid squares) and (0.00 2mol%) $Dy^{3+}$ (open circles) after a dose of 2Gy.**

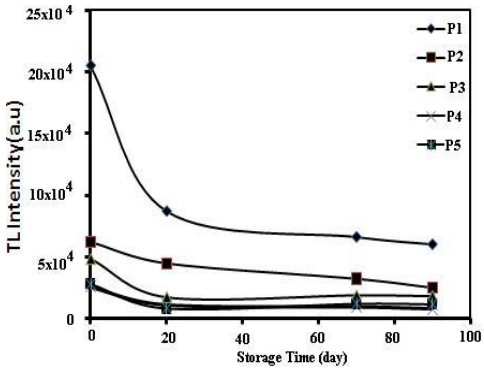


**Fig. 13. Fading characteristics of the silica glass samples doped with Dy(0.002 mol%). Samples are irradiated to 2Gy, annealed at $1100^oC/2h$ and storage at $18^oC$.**

## 4. CONCLUSIONS

Thermoluminescence in $SiO_2$ doped $Eu^{3+}$ and $Dy^{3+}$materials were successfully synthesized using the sol-gel technique. Its simple glow curve shows three obvious TL peaks of doped with the presence of overlapping types luminescence centers are formed. TL peaks intensities are dependent on concentration of $Eu^{3+}$ and $Dy^{3+}$ doping in the host material in all the samples. Similarly the peak intensity increases with β-ray dose up to 2Gy and then it becomes saturated after 2Gy β-rays exposure in all the materials, the temperature at maximum increases linearly with heating rate and the high temperature dosimetric peaks at 460-590K along with its little fading make the material suitable for radiation dosimetry at high temperature. The electrons are trapped in intermediate trap centers, which are mostly oxygen defects and, dopants present on surface.

## ACKNOWLEDGEMENTS

We would like to thank the Deanship of Scientific Research at the University of Jordan for providing financial support.

## COMPETING INTERESTS

Authors have declared that no competing interests exist.

## REFERENCES

1. Digonnet, M.J.F. Rare-earth-doped fiber lasers and amplifiers. 2nd ed. Marcel Dekker, NewYork; 2001.
2. Weber MJ. Science and technology of laser glass. J. Non-Cryst. Solids. 1990;123(1-3):208-222.
3. Han X, Cao G, Pratum T, Schwartz DT, Lutz B. Synthesis and properties of $Er^{3+}$-doped silica glass by sol-gel processing

with organic complexation. J. Mater. Sci. 2001;36(4):985-993.

4. Natalia IK, Viana B, Sanchez C. Rare-earth doped hybrid siloxane-oxide coatings with luminescence properties. J. Mater. Chem. 1993;3(1):111-112.
5. Thomas IM, Payne SA, Wilke GD. Optical properties and laser demonstrations of Nd-doped sol-gel silica glasses. J. Non-Cryst. Solids. 1992;151(3):183-194.
6. William VM, Jean-Luc RN, Robert HK. Preparation, processing, and fluorescence characteristics of neodymium-doped silica glass prepared by sol-gel process. J. Non-Cryst. Solids. 1990;121(1-3):267-272.
7. Lee LL, Tsai DS. Ion clustering and crystallization of sol-gel-derived erbium silicate glass. Jo. Mater. Sci. Lett. 1994;13(8):615-617.
8. Hess PC. The role of high field strength cations in silicate in silicate melts, in Physical Chemistry of Magmas, Advances in Physical Geochemistry. 1991;9:152-191.
9. Yusoffa AL, Hugtenburgb RP, Bradley DA. Review of development of a silica-based thermoluminescence dosimeter. J. Radi. Phys. and Chem. 2005;74:459-481.
10. Vedda A, Chiodini N, Di Martino D, Fasoli M, Griguta L, Moretti F, Rosetta E. Thermally stimulated luminescence of Ce and Tb doped $SiO_2$ sol-gel glasses. J. of Non-Crystalline Solids. 2005;351:3699-3703.
11. Pandey A, Sahare P, Shahnawaz D, Kanjilal D. Thermoluminescence and photoluminescence characteristics of sol-gel prepared pure and europium doped silica glasses. J. Phys. D: Appl. Phys. 2004;37:482-846.
12. Martini M, Spinolo G, Vedda A. Thermally stimulated luminescence of thermally grown $SiO_2$ films. Radiat. Eff. 1987;105:107.
13. Martini M, Spinolo G, Vedda A, Arena C. Phosphorescence and thermoluminescence of amorphous $SiO_2$. Solid State Commun. 1994;9(9):751.
14. McKeever SWS. Thermoluminescence of Solids. Cambridge University Press, Cambridge; 1985.
15. Susa K, Matsuyama I, Satoh S, Suganuma T. New optical fiber fabrication method. Electron. Lett. 1982;18(12):499-500.
16. Susa K, Matsuyama I, Satoh S, Suganuma T. Sol-gel derived Ge-doped silica glass for optical fiber application: I. Preparation of gel and glass and their characterization. J. Non-Crystalline Solids. 1990;119(1):21-28.
17. Susa K, Matsuyama II, Satoh S, Suganuma T. Sol-gel derived Ge-doped silica glass for optical fiber application: I. Preparation of gel and glass and their characterization. J. Non-Crystalline Solids. 1991;128(2):118-125.
18. Matsuyama I, Susa K, Satoh S, Suganuma T. Synthesis of high purity silica glass by sol-gel method. Am. Cream. Bull. 1984;63:1408-1411.
19. Mukasa K, Ono H, Wakabayashi R, Ishii K, Ohki Y, Nihikawa H. Luminescence properties of sol-gel synthesized silica glass induced by an ArF excimer laser. Phys. D: Appli. Physics. 1997;30:283.
20. Thermo Electron Corporation, Radiation Measurement & Protection, 26400 Broadway Ave. Oakwood Village, Ohio 44146 USA Thermo Suite, Thermo Electron Corporation RM&P ISO 9001 Quality System Certified, Model 3500 Manual TLD Reader with WinREMSTM, Operator's Manual.

    Available: http://www.thermo.com\rmp
21. Khames F. Synthesis and characterization of thermoluminescence properties of as prepared and doped $SiO_2$- glass. Ph.D. Thesis, The University of Jordan, Physics Department, Amman, Jordan; 2014.
22. Khamis F, Arafah DE. Thermoluminescence characteristics of natural quartz and synthesized silica glass prepared by sol-gel technique. AJOPACS. 2017; 3(1):1-16.
23. Townsend PD, Jazmati AK, Karali T, Maghrabi M, Raymond SG, Yang B. Rare-earth-size effects on thermoluminescence and second harmonic generation. J. Phys. Condens. Matter. 2001;13:2211-2224.
24. Raymond SG, Townsend PD. The influence of rare earth ions on the low-temperature thermoluminescence of $Bi_4Ge_3O_{12}$. J. Phys. Condens. Matter. 2000;12: 2103-2122.
25. Maghrabi M, Townsend PD. Thermoluminescence spectra of rare earth doped Ca, Sr and Ba fluoride. J. Phys. Condens. Matter. 2001;13 :5817-5831.

26. Akselrod MS, Agersnap Larsen N, Whitley V, McKeever SWS. Thermal quenching of F centre luminescence in $Al_2O_3$:C. J. Appl. Phys. 1998;84(6):3364-3373.
27. Zaragoza EC, González PR, Azorín J, Furetta C. Heating rate effect on thermoluminescence glow curves of LiF: Mg, Cu, P + PTFE phosphor. Appl. Radiat. Isot. 2011;69:1369-1373.
28. Piters TM, Bos AJJ. A model for the influence of defect interactions during heating on thermoluminescence in LiF: Mg, Ti (TLD-100). J. Phys. D: Appl. Phys. 1993;26:2255-2265.
29. Magharabi M, Arafah DE, Barham L, Olaimi M. The effect of rare earth doping on the glow peak positions of $LiNaSO_4$. J. Rad. Meas. 2007;42:163-169.



*Peer-review history:*
*The peer review history for this paper can be accessed here:*
*http://sciencedomain.org/review-history/21153*